dispersion management [19] or quasi-continuous filtering [20]. Proper dispersion management can be also introduced to extend Mamyshev's technique [21], for multi-wavelength operation [22,23]. Recently, the principle was applied in a polarization maintaining fiber, with bidirectional propagation, to regenerate four channels simultaneously [24]. On the other hand, PSAs have demonstrated multi-wavelength performance only as linear low noise amplifiers achieving sub 3 dB noise figure performance, with a single pump non-degenerate FWM based scheme [25].

Recently, we experimentally reported simultaneous phase regeneration on two 42.66 Gbit/s DPSK input signals using a phase sensitive amplifier (PSA) that is based on multi-pump degenerate four-wave mixing (FWM) [26]. In this paper, the PSA construction as a "black-box" subsystem and use as an in-line module is discussed along with details of the device optimization. Our scheme offers independent processing of each signal wavelength using a single nonlinear medium. Performance evaluation with periodic input phase distortion showed improvement in terms of receiver sensitivity by more than 10 dB, for both channels.

2. Principle and experiment setup

The experimental setup of the proposed regeneration scheme is illustrated in Fig. 1. At the input we have considered two independently modulated DPSK signals at 42.66Gbit/s. Each signal was produced by modulating separate laser sources, at 1549.91 nm and 1550.71 nm, with de-correlated pseudorandom binary sequences (PRBS) of 2^{31}-1 pattern length encoded using separate Mach Zehnder modulators. Pure phase distortion was added to both channels using a single phase modulator driven by a 14 GHz square wave from an independent device. The two channels were subsequently amplified to 14 dBm by an Erbium doped fibre amplifier (EDFA) and launched into the phase regenerator.

An in-line or "black-box" PSA based regenerator requires phase synchronization of its local pumps to the incoming signals. The synchronization stage should involve extraction of the signal carrier phase, translation to the required pump wavelengths and subsequent phase locking of the various signals [27]. The two DPSK channels were combined with a strong CW pump signal at 1547.91 nm. The three signals were amplified to a total power of 30 dBm and launched into a highly nonlinear fibre (HNLF). The HNLF used in this section was a strained aluminous-silicate highly nonlinear fibre whose increased stimulated brillouin scattering (SBS) threshold alleviated the need for active SBS suppression. The fibre had a length of 192 m and at 1550 nm the dispersion parameter was −0.2 ps/(nm·km), the nonlinear coefficient 7.4 $W^{-1}\cdot km^{-1}$ and the attenuation 14 dB/km. The optical spectrum at the output of the HNLF, taken at point B, is depicted in Fig. 1(b). The FWM interaction of the pump signal with each one of the two DPSK channels extracted a corresponding modulation stripped carrier at symmetric wavelength position. Each of the extracted carriers was self-locked to its data signal and the common local pump, maintaining the required frequency condition for PSA performance among the interacting waves [16,28].

After the carrier extraction stage the signal was split, and in one path, the generated carriers were selected by an optical filter and were used to optically injection lock two additional local pump lasers. The injected power of each carrier was kept below −35 dBm, at a level where the limited bandwidth (< 0.5 GHz) of the injection locking process rejected any residual phase modulation on the input signal [29]. Operating the synchronization units at such low bandwidths is a necessary condition for a black-box PSA to achieve broadband phase noise suppression [30].The emitted power of each local pump laser was 8 dBm. The two injection locked pump lasers from one path and the signal and common pump from the other were directed to a wavelength selective switch (WSS). The WSS suppressed the unwanted spectral components that had been generated from the FWM process in the carrier extraction stage, see Fig. 1(b). The filtered spectrum at the output of the WSS is depicted in Fig. 1(c). It includes the common CW pump (pump 1), the two propagated DPSK signal channels and their corresponding phase locked CW pump waves (pump 2, pump 3) at the symmetric wavelength positions of 1551.91 nm and 1553.52 nm, respectively.

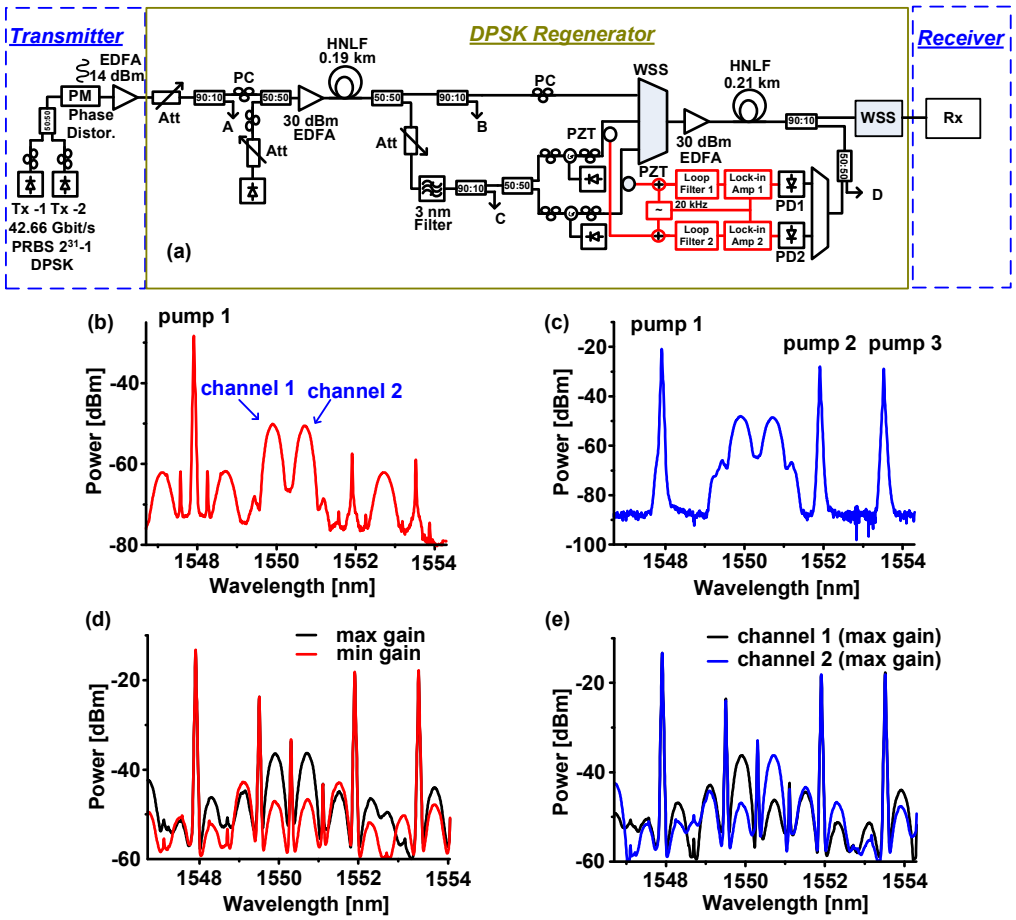

Fig. 1. (a) Experimental setup of the two channels PSA based phase regenerator for BPSK signals. (b) Optical spectrum after the carrier extraction stage; (Tx: transmitter, PC: polarization controller, Att: attenuator, PD: photodiode, Rx: receiver). (c) Optical spectrum at the input of the 2nd HNLF. (d) Optical spectrum at the output of the 2nd HNLF (point D) when both channels are locked either at the maximum or minimum phase sensitive gain state of the PSA. (e) Optical spectrum at the output of the 2nd HNLF (point D) when the channels are locked at different phase sensitive gain states of the PSA

After the WSS the combined signals were amplified to 30 dBm and launched into a second HNLF for the phase sensitive regeneration process, which was similar to the fibre of the carrier extraction stage but with a length of 210 m. The interferometric nature of the scheme made it vulnerable to slow temperature induced path length variations which accordingly affected the phase sensitive gain of the PSA. Since the input DPSK channels were not phase correlated and their corresponding pumps, out of the injection locking process, followed different paths in the interferometer, separate compensation against phase drifts was provided. This was achieved with a feedback circuit setup that used both channels at the output of the PSA as error signals to control two different piezoelectric fibre stretchers (PZTs), one for each pump path. A 20 kHz dithering tone was added onto the control signals of the PZTs, and subsequently extracted with corresponding lock-in amplifiers, in order to lock each channel at the maximum or minimum phase sensitive gain states of the PSA. Figure 1(d) depicts the resulting spectra at the output of the regeneration stage of the PSA, taken at point D, when the channels were simultaneously locked at the maximum or minimum phase sensitive gain, respectively. A gain contrast ratio of 11 dB was achieved for both channels.

#155921 - $15.00 USD Received 3 Oct 2011; revised 4 Nov 2011; accepted 8 Nov 2011; published 9 Dec 2011

Figure 1(e) depicts the output spectra when the two channels were locked at two different phase sensitive gain states.

The interaction of the three pumps in the HNLF created strong FWM products that could potentially overlap with the incoming signals. To avoid such scenario a careful selection of the pump wavelengths with respect to the incoming signal locations was required, see Fig. 1(d),(e). More specifically, the frequency distance of the common pump with each signal should be a non-integer multiple of their channel spacing. Additional data signals from the Bragg scattering and phase conjugation processes within the HNLF were created, spanning a large wavelength spectrum. A final WSS was required at the output of the PSA to select the two signals and remove the unwanted wavelengths. Finally, at the receiver section an 1-bit delay interferometer was used for demodulating the channels. The output of the interferometer was connected to a balanced photodiode and phase locked loop clock recovery circuit for detecting the signal and for performing the BER analysis.

3. Results

The high complexity of the system required rigorous optimization of each stage to maximize the overall performance. At the carrier extraction stage the optimum power level of the local pump with respect to the power of the input signal had to be optimized so that the carriers could be extracted without degrading the signal quality. This was achieved by measuring the bit error rate (BER) of both channels at the output of the 1st HNLF and characterizing the penalty in their received sensitivity (defined at BER: 10^{-9}) as a function of the pump-to-signal power ratio $P_{pump1}/P_{channel(n)}$, where P_{pump1} is the power level of the pump-1 and $P_{channel(n)}$ (n = 1, 2) the power level of either of the two DPSK channels, $P_{channel(1)} = P_{channel(2)}$, measured also at the output of the 1st HNLF. The results of this analysis are depicted in Fig. 2. The power level of the EDFA at the input of the HNLF was always kept constant and equal to 30 dBm, therefore, lower values of the pump-to-signal power ratio effectively corresponded to higher launched signal powers. This caused degradations due to inter-channel nonlinearities and led to penalties that approached 2 dB. The penalty was reduced to less than 0.5 dB when the pump-to-signal power ratio became larger than 3 dB. For the remainder of our study this ratio was set at 10 dB.

At the second stage of the PSA two critical parameters had to be optimized, namely, the powers of the local pumps as well as the relative level of the signal power with respect to the pumps. We characterized the sensitivity penalty of the two channels at the output of the PSA by varying both parameters with the help of the first WSS, see Fig. 3(a-b). In addition, we evaluated the phase suppression capabilities of the PSA by measuring the introduced improvement in terms of receiver sensitivity when the input channels were distorted by 3 dB at the input of the PSA.

Figure 3(a) shows the measured penalty for both channels as a function of the ratio of the pump-1 power P'_{pump1} to the power level $P'_{pump(n)}$ (n = 2, 3) of either of the two pump waves (pump −2, pump −3), i.e. $P'_{pump1}/P'_{pump(n)}$, where $P'_{pump(2)} = P'_{pump(3)}$. These power levels were measured at the output of the 2nd HNLF fibre, whilst at its input an EDFA set the power to a constant total level of 30 dBm. The common pump (pump-1) interacted with pump-2 and pump-3, therefore at low power ratios it was strongly depleted. As a result, the effective noise figure of the PSA was degraded and an additional sensitivity penalty was introduced. On the other hand, when pump 1 became too large the phase sensitive gain of the amplifier was reduced due to the low power of pumps 2 and 3. The optimum operating region was achieved for pump-to-pump power ratios of around 5 dB, where the sensitivity penalty was less than 0.5 dB for both channels. Subsequently, the two channels were subjected to phase distortion, which degraded their received sensitivities at the input of the PSA by 3 dB. The PSA improved the channels' performance by suppressing the distortion. The corresponding improvement in receiver sensitivity was defined as regeneration and it has been measured for both channels as a function of the pump-to-pump power ratio, see Fig. 3(a). Best performance occurs at the optimum operating point of the undistorted case, where the regeneration approaches 2 dB.

#155921 - $15.00 USD Received 3 Oct 2011; revised 4 Nov 2011; accepted 8 Nov 2011; published 9 Dec 2011

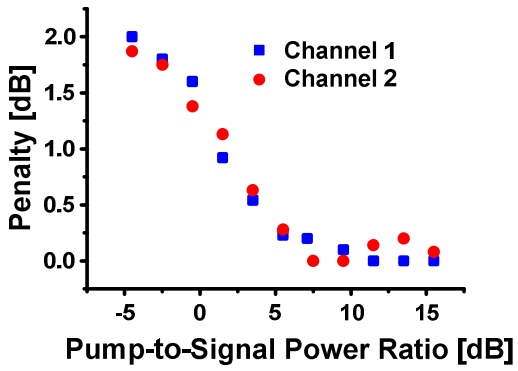

Fig. 2. Receiver sensitivity penalty (@ BER: 10^{-9}), with respect to back-to-back performance, measured for both channels at the output of the carrier extraction stage as a function of the pump-to-signal power ratio as appears at the same output. Penalty less than 0.5 dB is achieved when the power ratio becomes larger than 3 dB.

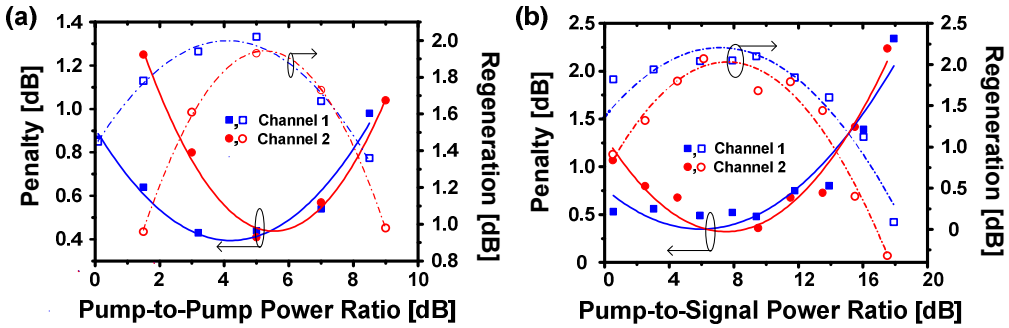

Fig. 3. Receiver sensitivity penalty or improvement with respect to back-to-back performance measured for both channels at the output of the PSA, (a) as a function of the pump-to-pump power ratio for undistorted channels at the PSA input as well as when they have experienced 3 dB penalty due to phase distortion, (b) as a function of the pump-to-signal power ratio for undistorted channels at the PSA inputs well as when they have experienced 3 dB penalty due to phase distortion.

Having optimized the pump power profile of the PSA the next step was to identify the optimum power level of the two signals. The results of this optimization process are depicted in Fig. 3(b). More specifically, the figure shows the sensitivity penalty for both channels as a function of the ratio of the pump-1 power P'_{pump1}, to the power level of either of the two DPSK signals $P'_{channel(n)}$ (n = 1, 2) i.e. $P'_{pump1}/ P'_{channel(n)}$, where $P'_{channel(1)} = P'_{channel(2)}$These power levels were defined at the output of the 2nd HNLF. At low ratios the signal power level effectively increased and the regenerator operated under saturation. This gave rise to stronger nonlinear interactions between the two data signals as well as among the data signals and the common pump-1, which degraded by a relatively small amount the performance of the PSA. However, much higher penalties appeared when the pump-to-signal power ratio was set beyond 12 dB. This was due to the excess signal attenuation that was required by the WSS to set this power ratio and which increased the effective noise figure of the PSA. The optimum point appeared at the value of 8 dB, and resulted in a penalty of 0.5 dB. The figure shows also the results of a similar optimization process when the input channels have experienced a phase degradation that corresponded to 3 dB sensitivity penalty at the input of the PSA. At the optimum operating point a sensitivity improvement of 2 dB was achieved for both signals.

#155921 - $15.00 USD Received 3 Oct 2011; revised 4 Nov 2011; accepted 8 Nov 2011; published 9 Dec 2011

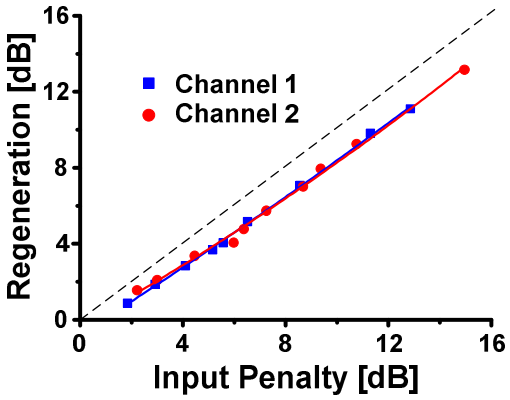

Fig. 4. Receiver sensitivity improvement with respect to back-to-back performance measured for both channels at the output of the PSA as a function of the input penalty caused by different strengths of introduced phase distortion

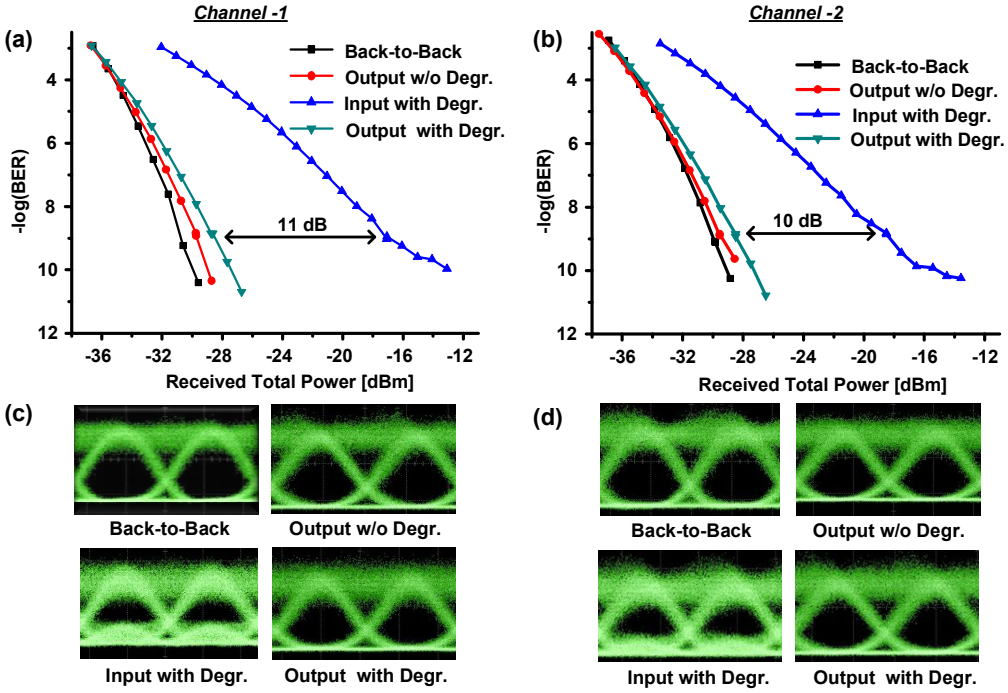

Fig. 5. BER measurements versus total received power (a) for channel 1 and (b) for channel 2 at input/output of PSA with/without the presence of input periodic degradation. Corresponding eye diagrams (c) for channel 1 and (d) for channel 2

We finally assessed the regenerative capabilities of the PSA against various levels of input phase distortion, as shown in Fig. 4. Despite the presence of a small offset attributed to OSNR degradation and inter-channel crosstalk, Fig. 4 demonstrates that the achieved regeneration nearly tracks the penalty induced by the phase distortion, offering over 10 dB improvement in the receiver sensitivity, when the applied phase distortion induces a 12 dB penalty. Figure 5(a)-(b) depict measured BER curves for both channels taken against total received power, for input degradations of about ~10 dB at 10^{-9}. It is also shown that in the absence of any input degradation the receiver sensitivity penalty of each channel at 10^{-9} was less than 1 dB, and error free operation was achieved. Furthermore, when introducing significant phase distortion

#155921 - $15.00 USD Received 3 Oct 2011; revised 4 Nov 2011; accepted 8 Nov 2011; published 9 Dec 2011

on the input channels, the PSA demonstrated the anticipated phase squeezing capabilities. The restored eye diagrams are illustrated in Fig. 5(c) and Fig. 5(d). Although balanced detection has been used, the monitored eye diagrams refer only to the duo-binary output of the one-bit delay interferometer. Therefore they are asymmetric and their upper rails carry more noise with respect to the lower rails as they result from signal-to-spontaneous emission beating at the photodiode. However, considering this asymmetry, we believe that both rails are regenerated. Finally, we have to point out that if random phase noise is considered at the input, the regenerative performance of the PSA is expected to be less efficient. This could be attributed partially to a non-fragmented distribution of the introduced phase noise [30], as well as to an enhanced amplitude distortion from phase-to-amplitude conversion in the HNLF [18].

4. Conclusions

We have proposed and experimentally implemented, for the first time to our knowledge, an in-line PSA with multichannel regenerative capabilities. The regenerative performance of our scheme has been evaluated against periodic phase distortion on two 42.66 Gbit/s DPSK signals. Significant recovery of the undistorted signal quality has been achieved for both channels, quantified by more than 10 dB improvement in terms of receiver sensitivity.

Acknowledgments

This work has been supported and by European Communities Seventh Framework Programme FP/2007-2013 under grant agreement 224547 (PHASORS) and by Science Foundation Ireland under Grant 06/IN/I969

#155921 - $15.00 USD Received 3 Oct 2011; revised 4 Nov 2011; accepted 8 Nov 2011; published 9 Dec 2011